A Local ROI-specific Atlas-based Segmentation of Prostate Gland and Transitional Zone in Diffusion MRI

Junjie Zhang[1], Sameer Baig[1], Alexander Wong[2], Masoom A. Haider[1], Farzad Khalvati[1]
[1] Sunnybrook Research Institute, Medical Imaging, University of Toronto, Toronto, ON, Canada
[2] Systems Design Engineering, University of Waterloo, Waterloo, ON, Canada

Introduction

Segmentation of prostate and related anatomic structure, such as transitional zone, in medical images facilitates prostate cancer detection, as well as a number of other clinical practices.

- Usually the first step in computer-aided detection of prostate cancer.

The current practice of manually contouring the prostate gland in MR images is a tedious task.

- Computer-assisted segmentation methods could reduce the time spent manually contouring the prostate gland and potentially reduce the inter-user variability of diagnosis.

Related Researches

A popular class of algorithms in literature for prostate segmentation is *atlas-based segmentation* (ABS) algorithms [1].

In ABS, registration between atlas images and the target image, in particular for MR images, can be difficult:

- Large variability of the MR images in terms of image intensity characteristics (e.g. scanner variability)
- Structure (e.g., different field of views (FOVs) and different imaging center), and anatomical variabilities of scanned regions.

Method

We propose a semi-automatic *local ROI-specific atlas-based segmentation* (LABS) method to segment prostate gland and transitional zone in diffusion MR images (Figure 1), inspired by ABS and a *sequential registration-based segmentation* (SRS) method [2]:

- Minimize user interaction;
- Focus on the vicinity of prostate for atlas matching and atlas-to-target registration;

Step I: User-specified Bounding Box

- The user specifies the bounding boxes (BBs) of the prostate gland on key slices (e.g., the base, middle, and the apex);
- Enlarged BBs are interpolated across slices to produce the prostate volume of interest (VOI).

Step II: Atlas Selection

- Corresponding prostate VOIs are extracted from atlas database w.r.t. the prostate VOI of target patient;
- Best matched VOI is then selected from atlas based on two criteria: the similarity measurement and volume ratio.

Step III: ROI-based Registration

- Similar to ABS, best matched VOI is registered to target VOI using an affine registration method.

Step IV: Transformation and Post-processing

- Mask VOI in atlas is then transformed and scaled to the size of interpolated BBs to produce segmentation for both prostate and transitional zone.

* The pipeline is implemented in ProCanVAS.

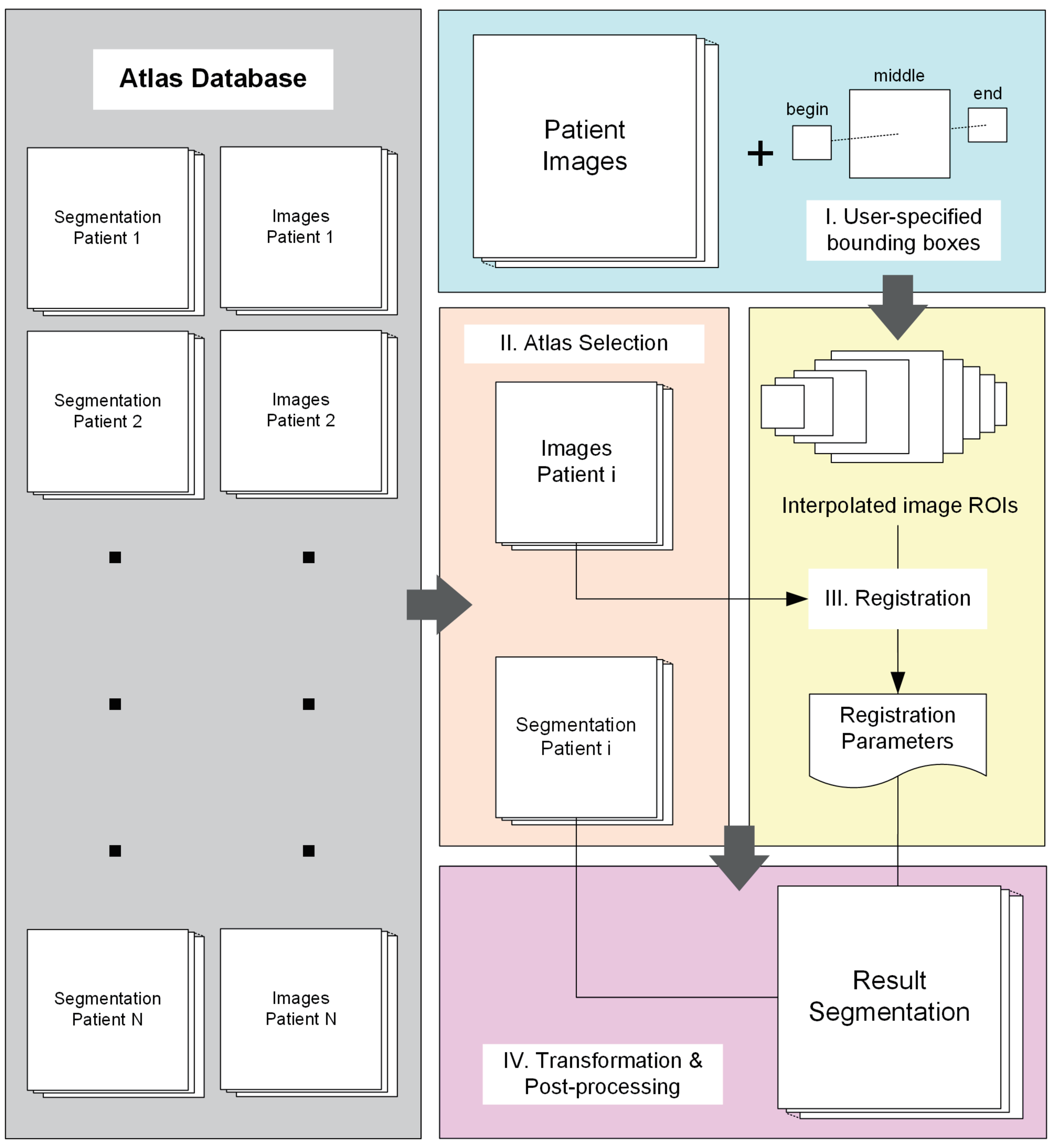

Figure 1: The proposed local ROI-specific atlas-based segmentation (LABS) pipeline. Each step is highlighted in blocks with different colors.

Results and Conclusion

The algorithm was validated on diffusion MRIs of 100 patients using leave-one-out method*.

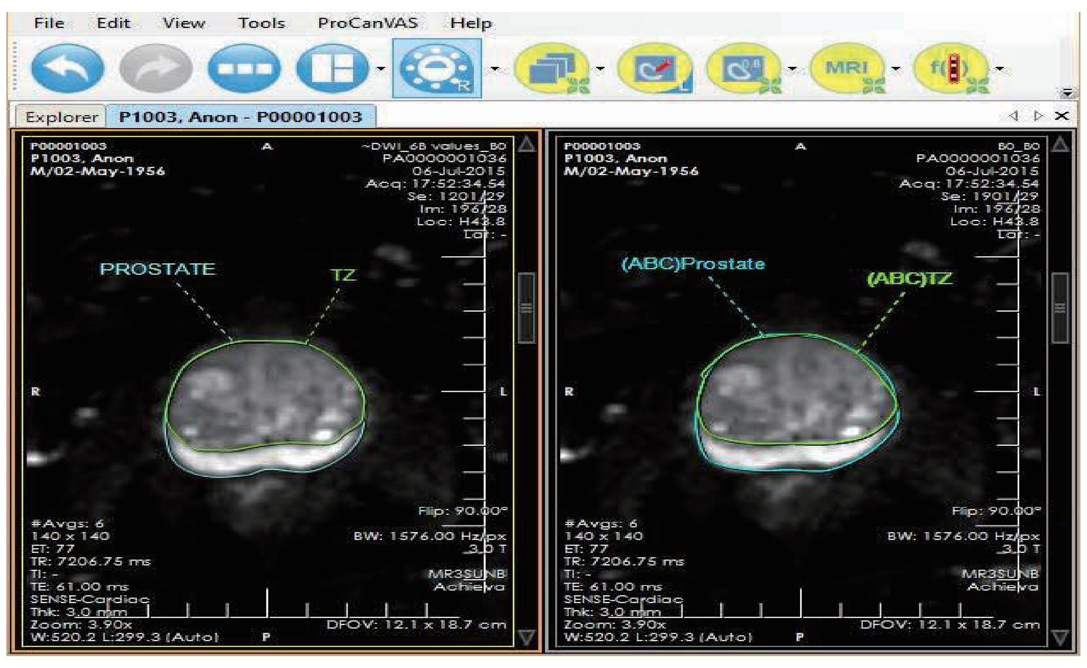

Quantitative Analysis

Tables 1, 2 and Figure 2 present results with both 3 and 5 user-specified bounding boxes, and the segmentation results with (w.) and without (w/o. or original) post-processing, by Dice Similarity Coefficient (DSC).

Table 1. DSC (%) of prostate gland segmentation.

	3 BBs	5 BBs	$\overline{\Delta DSC}$
w/o. post-processing	**76.8**±8.2	**78.3**±6.5	*+1.5*
w. post-processing	**80.2**±4.7	**85.4**±3.2	*+5.2*
$\overline{\Delta DSC}$	*+3.4*	*+7.1*	

Table 2. DSC (%) of transitional zone segmentation.

	3 BBs	5 BBs	$\overline{\Delta DSC}$
w/o. post-processing	**69.1**±9.6	**70.6**±8.4	*+1.5*
w. post-processing	**73.7**±6.8	**77.3**±5.9	*+3.6*
$\overline{\Delta DSC}$	*+4.6*	*+6.8*	

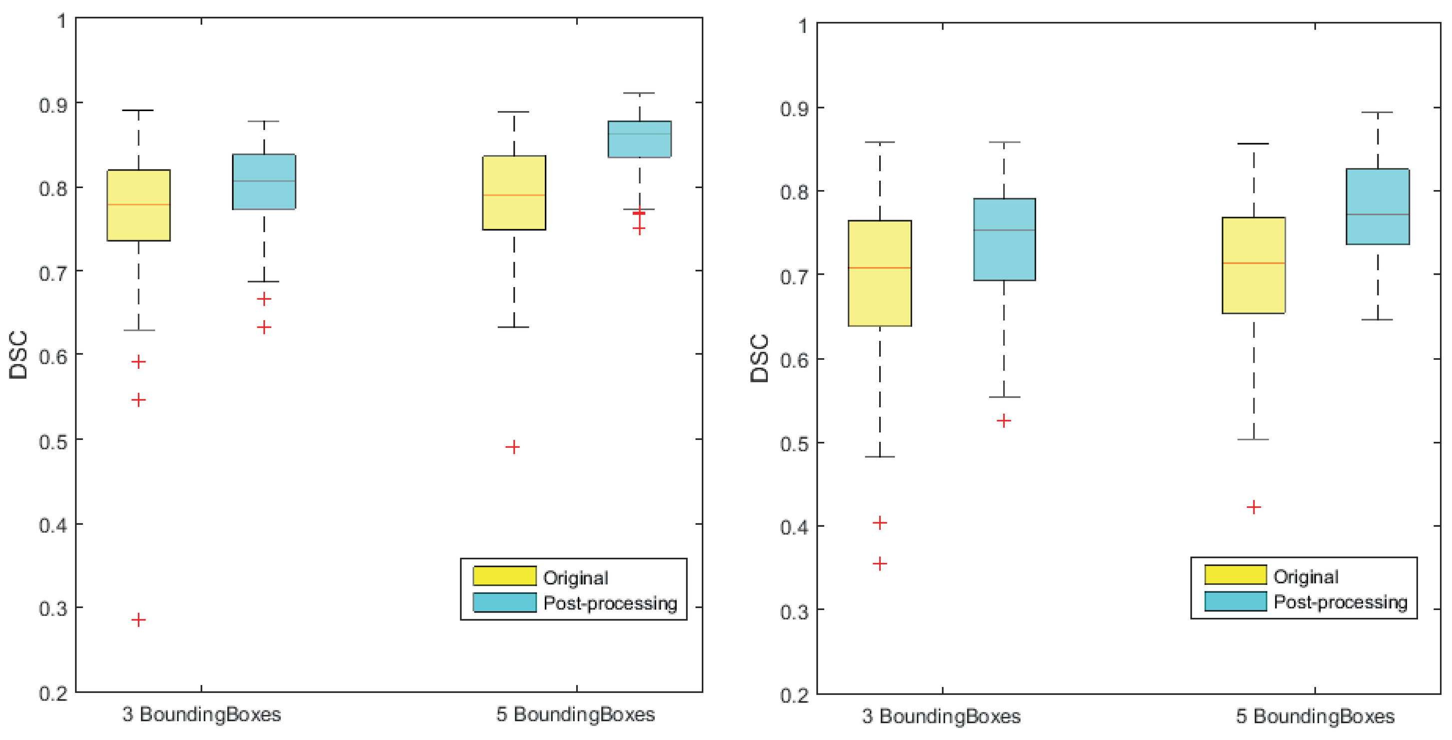

Figure 2: Results (DSC) for prostate gland (left) and transitional zone (right) segmentation.

[1] Klein, S. et al., (2008). Automatic segmentation of the prostate in 3D MR images by atlas matching using localized mutual information. Medical Physics, 35(4), 1407–1417

[2] Khalvati, F., et al., (2016). Sequential Registration-Based Segmentation of the Prostate Gland in MR Image Volumes. Journal of Digital Imaging, 29(2), 254–263.